Morphological Diversity and Transcriptomic Profiling of Multicellular Trichomes in Kiwifruit

Xiaoqiong Qi †, Fei Han †, Lansha Luo †, Haiyan Lv, Yanqing Deng, Edmore Gasura, Changsheng Xiao, Xianzhi Zhang, Yinghua Deng *, Xiaodong Xie *

Posted Date: 28 January 2026

doi: 10.20944/preprints202601.2058.v1

Keywords: *Actinidia*; trichome morphogenesis; pericarp anatomy; polyploidization; transcriptomics

 doi:10.20944/preprints202601.2058.v1

Article

Morphological Diversity and Transcriptomic Profiling of Multicellular Trichomes in Kiwifruit

Xiaoqiong Qi [1,†], Fei Han [2,†], Lansha Luo [3,†], Haiyan Lv [2], Yanqing Deng [4], Edmore Gasura [5], Changsheng Xiao [1], Xianzhi Zhang [3], Yinghua Deng [1,*] and Xiaodong Xie [2,5,*]

[1] Hubei Key Laboratory of Purification and Application of Plant Anti-cancer Active Ingredients, Hubei University of Education, Wuhan 430205, China

[2] Wuhan Botanical Garden, Chinese Academy of Sciences, Wuhan 430074, China

[3] Zhongkai University of Agriculture and Engineering, 24 Dongsha Street, Haizhu District, Guangzhou City, Guangdong Province, 510225, China

[5] Wuhan Agricultural Inspection Center, Wuhan, China

[4] China-Zimbabwe Belt and Road Joint Laboratory on Agricultural Ecology and Cash Crops, Wuhan Botanical Garden, Chinese Academy of Sciences, Wuhan 430074, China

* Correspondence: xxd0624@sina.com, dengyinghua@hue.edu.cn

† These authors contributed equally.

Abstract

Fruit trichomes and pericarp architecture are pivotal for biological defense and postharvest resilience in the genus *Actinidia*. However, the evolutionary diversity of these structures and the molecular mechanisms governing their development—particularly under the influence of polyploidization—remain poorly understood. We performed a systematic evaluation of 21 *Actinidia* species and 14 cultivars using scanning electron microscopy (SEM) and histological analysis. To determine the effects of genome doubling, an autotetraploid line was induced from diploid *A. chinensis* cv. 'Donghong', followed by comparative transcriptomic and temporal expression profiling. Morphological characterization identified three distinct evolutionary groups based on fruit surface traits: glabrous, caducous-spotted, and persistent-pubescent. All observed trichomes featured a unique bipartite multicellular architecture. Kiwifruit pericarp thickness (59.8–534.6 μm) was locally reinforced at trichome insertion sites. Among kiwifruit cultivars, polyploidization significantly increased both trichome length and total amount. Transcriptomic analysis revealed 235 differentially expressed genes (DEGs) enriched in hormonal signaling and flavonoid pathways. Two key candidate genes, *Achv4p15g023764.t1* and *Achv4p01g000003.t1*, were identified as candidate gene for stage-specific regulators governing early morphogenesis and late maturation. These findings provide a structural roadmap of *Actinidia* epidermal evolution and identify specific genetic targets for the molecular breeding of cultivars with optimized surface protection and postharvest resilience.

Keywords: *Actinidia*; trichome morphogenesis; pericarp anatomy; polyploidization; transcriptomics

1. Introduction

Plant trichomes, or epidermal hairs, are specialized uni- or multicellular appendages arising from the aerial epidermis, functioning as a critical interface between the plant and its environment [1,2]. Morphologically, these structures are broadly categorized into non-glandular trichomes (NGTs) and glandular secretory trichomes (GSTs) [2]. NGTs primarily provide physical protection by reflecting ultraviolet radiation, mitigating transpiration, and physically obstructing herbivore movement [3,4]. In specialized cases, such as the desert-dwelling *Agriophyllum squarrosum*, dendritic NGTs facilitate non-stomatal water movement—a critical adaptation for survival in arid climates [4]. Conversely, GSTs act as metabolic "bio-factories," synthesizing and sequestering high-value

 doi:10.20944/preprints202601.2058.v1

secondary metabolites—such as artemisinin in *Artemisia annua*—to form a potent chemical defense layer against pathogens and pests [5,6].

In horticultural science, fruit surface trichomes are of significant economic importance, directly influencing fruit aesthetics, post-harvest shelf life, and consumer preference [7,8]. While extensively studied in model crops like tomato, research regarding the diverse trichome architectures within the genus *Actinidia* (kiwifruit) remains sparse [9]. *Actinidia*, a genus native to China comprising 75 taxonomic units [10], is globally renowned as the "king of Vitamin C". The genus exhibits an extraordinary spectrum of fruit surface morphologies—ranging from glabrous to densely pubescent or lenticulate—which serves as a fundamental marker for species differentiation. Historically, *Actinidia* has been classified into four sections based on these traits: *Leiocarpae*, *Maculatae*, *Strigosae*, and *Stellatae* [11]. This phenotypic diversity, spanning from the smooth epidermis of *A. arguta* to the rigid bristles of *A. chinensis* var. *hispidus*, provides a robust evolutionary model for investigating the relationship between trichome morphogenesis and pericarp architecture.

Recent advancements in molecular biology have elucidated the complex regulatory networks governing trichome morphogenesis [2,5]. In multicellular systems, HD-Zip IV transcription factors, such as the Woolly (Wo) gene and homeodomain–leucine zipper (HD-ZIP) genes in tomato, serve as master regulators of trichome initiation and self-pollination [12,13]. Furthermore, the identification of the MYC transcription factor module has highlighted a sophisticated regulatory switch that couples glandular trichome development with specialized metabolic flux [6]. Beyond classical transcriptional control, the epigenetic landscape—including the miR156-SPL module and m^6A RNA methylation—has been shown to fine-tune trichome density and metabolic output in response to developmental timing and environmental cues [14].

Despite these biological insights, *Actinidia* research has focused predominantly on genomic analysis [15], leaving a critical gap in the systematic characterization of trichome diversity and its structural integration with the pericarp. This study addresses this gap by evaluating trichome morphology and pericarp thickness across 35 diverse *Actinidia* accessions. By integrating high-resolution phenotypic data with transcriptomic profiling of ploidy-induced changes, we aim to elucidate the mechanisms underlying trichome development and genome doubling. These findings establish a theoretical framework for kiwifruit defense strategies and provide targeted molecular markers for breeding programs focused on optimizing fruit skin characteristics for the global industry.

2. Materials and Methods

2.1. Plant Materials and Sampling

Experimental plant materials were obtained from the National Kiwifruit Germplasm Repository at the Wuhan Botanical Garden, Chinese Academy of Sciences (Wuhan, China). Phenotypic evaluations were conducted from late June to late October (2023–2025) to capture the full spectrum of fruit development. The study cohort included 21 *Actinidia* species—representing all four taxonomic sections (*Leiocarpae*, *Maculatae*, *Strigosae*, and *Stellatae*)—and 14 commercial cultivars. The selected cultivars exhibited diverse trichome morphologies and varying ploidy levels (diploid, tetraploid, and hexaploid) to ensure a comprehensive representation of the genus.2.2.

2.2. Micromorphological Characterization of Trichomes

2.2.1. Optical and Stereomicroscopy

Fresh fruit skin samples (approximately 0.2×0.2 cm) were excised from the equatorial region of each fruit using surgical scalpels. Individual trichomes were isolated using fine-tipped forceps. Samples were mounted in deionized water on glass slides and initially screened using a Leica S9i stereomicroscope to assess overall distribution. High-resolution structural analysis, including branching patterns and cellular architecture, was performed using a Nikon Eclipse Ts2 inverted

 doi:10.20944/preprints202601.2058.v1

microscope (Nikon, Tokyo, Japan) at magnifications ranging from 20× to 400 x. All investigations were conducted with meticulous care to preserve the integrity of the trichome coverage, and each sampling was performed with no fewer than five replicates.

2.2.2. Scanning Electron Microscopy (SEM)

For ultrastructural analysis, skin samples (3×3mm) were fixed in FAA (Formalin-Aceto-Alcohol) at 4℃ for 24 h. Samples underwent graded ethanol dehydration (10% to 100%, v/v) and were dried using a Leica EM CPD300 critical point dryer (Leica Microsystems, Germany) with liquid CO_2 as the transitional fluid. Dried samples were mounted on aluminum stubs and sputter-coated with a 15-20 nm gold layer using a Model SBS-12 ion sputter coater. Observations were conducted using a Hitachi SU8100 SEM (Hitachi, Tokyo, Japan) at an accelerating voltage of 5-15 kV. Trichome density (hairs per unit area) was quantified across five random fields per sample using ImageJ software (v1.53, NIH, USA). All investigations were conducted with meticulous care to preserve the integrity of the trichome coverage, and each sampling was performed with no fewer than five replicates.

2.3. Histological Analysis of Pericarp Thickness

Pericarp thickness was determined using a modified paraffin sectioning protocol. Cylindrical cores (diameter: 5 mm containing the epidermis and outer flesh were extracted from three equatorial points per fruit. Samples were fixed in FAA, vacuum-infiltrated, and dehydrated through a graded ethanol-xylene series. Following infiltration with paraffin wax 58-60℃, 8 μm thick transverse sections were generated using a Leica RM2235 rotary microtome.

Sections were stained with Safranin O (1%) and counterstained with Fast Green FCF (0.5%). Digital slides were captured via a PANNORAMIC 250 automated scanner (3DHISTECH, Budapest, Hungary). Pericarp thickness—defined as the distance from the outer epidermis to the outermost parenchyma layer—was measured at ten random intervals per section using Saiviewer 2.4 software.

2.4. Assessment of Ploidy Levels

Ploidy levels were determined via flow cytometry (FCM). Young, expanding leaves were finely chopped in 0.5 mL of nuclear extraction buffer (High Resolution Kit, Partec, Germany) and filtered through a 30 μm nylon mesh (CellTrics™, Partec, Germany). Subsequently, 2 ml of a precooled (4 °C) staining solution containing 4',6-diamidino-2-phenylindole (DAPI; Solution B of the kit) was added. DNA content was quantified using a CyFlow Space flow cytometer (Partec, Germany). Only analyses with a coefficient of variation (CV) < 5% were considered valid. The diploid *A. chinensis* var. *chinensis* 'Hongyang' ($2n = 2x = 58$) served as the internal reference standard.

2.5. Transcriptomic Profiling and Bioinformatic Analysis

Total RNA was extracted from young leaves, petioles, and stems of diploid and autotetraploid ‘Donghong’ lines (three biological replicates) using a modified CTAB method. RNA quality was validated using an Agilent 2100 Bioanalyzer (Agilent Technologies, CA, USA). Strand-specific cDNA libraries were constructed and sequenced on the DNBSEQ platform (BGI, Shenzhen, China) using 150-bp paired-end chemistry. Raw reads were processed using fastp (v0.23.2) to remove adapters and low-quality bases (Q≤20 for >40% of bases). Clean reads were aligned to the *A. chinensis* ‘Hongyang’ 4.0 reference genome using HISAT2 (v2.2.1). Transcript assembly and quantification were performed via StringTie (v2.2.1). Differential expression analysis was conducted using the DESeq2 R package (v1.38.3). Differentially expressed genes (DEGs) were defined by $|\log_2(\text{Fold Change})| \geq 1$ and a False Discovery Rate (FDR)-adjusted *p*-value (*padj*) < 0.05. Functional annotation and enrichment analyses were performed using the GO and KEGG databases via Fisher's exact test. Expression analysis of candidate genes related to trichome traits was carried out using the Kiwifruit Transcriptome Database (KTD) (available at http://ktd.fruitomicshub.com/home/).

 doi:10.20944/preprints202601.2058.v1

2.6. Statistical Analysis

Data were processed using Microsoft Excel 2019 and analyzed with IBM SPSS Statistics 26.0. Normality and variance homogeneity were confirmed prior to one-way Analysis of Variance (ANOVA). Significant differences between means were determined using Duncan's Multiple Range Test (a = 0.05). Visualization was performed using Origin 2024.

3. Results

3.1. Morphological Diversity of Kiwifruit Epidermis and Trichomes

This study systematically characterized the pericarp and pubescence features of 21 *Actinidia* species and 14 commercial cultivars (Figure 1a). For comparative analysis, the materials were categorized into three taxonomic groups based on trichome morphology: Section *Leiocarpae*, Section *Maculatae*, and a combined Section *Stellatae*/*Strigosae* group. Morphological evaluation (Figure 1a) revealed that species within Sections *Leiocarpae* and *Maculatae* predominantly exhibit small-fruited phenotypes, with individual fruit weights ranging from 0.2 to 10 g and longitudinal diameters typically under 2 cm. Conversely, the *Stellatae*/*Strigosae* group displayed larger fruit sizes and highly heterogeneous trichome architectures. Microscopic and scanning electron microscopy (SEM) analyses (Figure 1b, c) identified distinct sectional patterns. Section *Leiocarpae* possesses a glabrous epidermis entirely devoid of pubescence, representing a primary genetic resource for the development of edible-peel cultivars. Section *Maculatae* characterized by a lenticulate (spotted) surface architecture with highly significant interspecific variation ($P < 0.001$) in spot density and size. For example, *A. callosa* var. *henryi* features a smooth epidermis with prominent spots, while *A. wantianensis* exhibits high-density, fine striations. Section *Stellatae*/*Strigosae* exhibits the most prolific and diverse trichome. Key commercial species such as *A. chinensis*, *A. deliciosa*, and *A. eriantha* reside here. Their pubescence is further differentiated into series: the *A. chinensis* series features fascicled short hairs that partially degenerate in later stages; the *A. deliciosa* series is dominated by fascicled long, rigid bristles (stiff-hair type) or individual stiff hairs with variable density (Figure 1b, c); and the *A. eriantha* series possesses a fascicled tomentose (soft-hair) type with extreme density, forming a contiguous physical barrier.

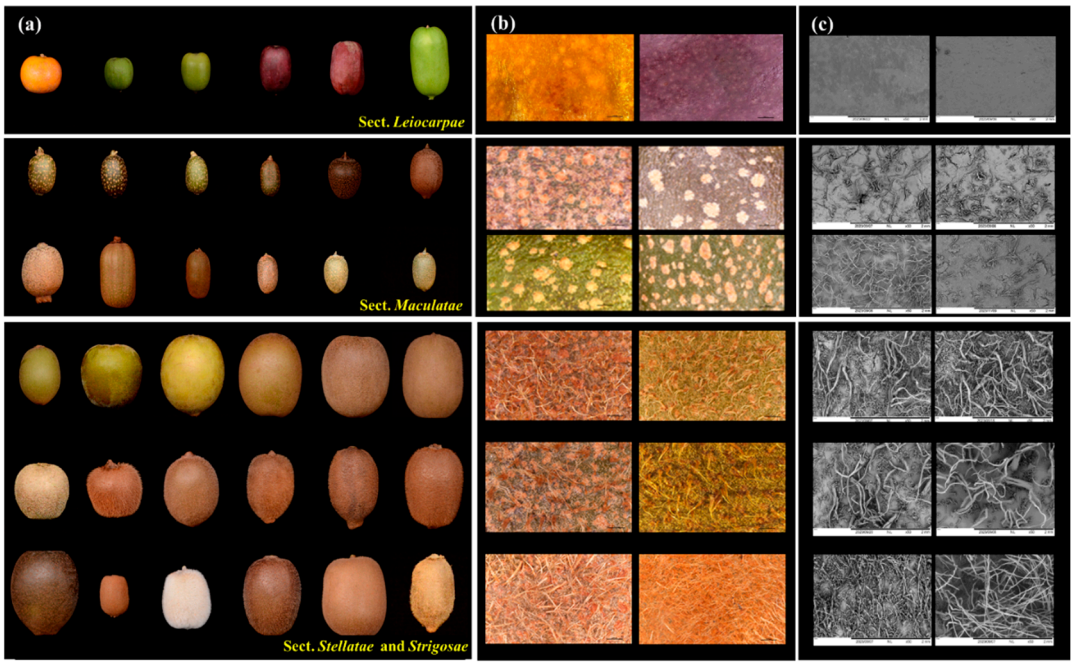

Figure 1. Fruit surface characteristics and microscopic observations in kiwifruit. (a) Diversity in fruit morphological traits among the Sect. *Leiocarpae*, Sect. *Maculatae*, and combined Sect. *Stellatae* and *Strigosae*

 doi:10.20944/preprints202601.2058.v1

groups. (b) Phenotypic characteristics of the fruit peel observed via microscopy. (c) Trichome morphology on fruits from the three groups investigated by scanning electron microscopy.

3.2. Cytological Architecture of Kiwifruit Multicellular Trichomes

Cytological profiling confirmed that all observed kiwifruit trichomes are non-glandular and possess a bipartite structure consisting of a basal cell region and an elongated stalk cell (Figure 2). The terminal stalk cells are typically acute and significantly elongated. No unicellular trichomes were identified across the 35 accessions, suggesting a high degree of functional specialization in the fruit trichome. There exist variations in the size and number of trichome cells among different species and cultivars of kiwifruit, leading to highly significant differences in trichome length, thickness, and overall volume between species. For instance, the trichome volume of *Actinidia eriantha* exceeds that of *Actinidia rufa* by more than tenfold. In the spotted-fruit group (Sect. *Maculatae*), the architecture is relatively rudimentary, typically comprising 1–3 basal cells connected to 2–6 short stalk cells (100 μm) with a tapered conical apex (Figure 2a). In species such as *A. hubeiensis* and *A. indochinensis*, the stalk cells exhibit developmental curling and premature degeneration into a single-branch state. In the pubescent group (*Stellatae*/*Strigosae*), cellular differentiation is more pronounced. In *A. chinensis*, dozens of basal cells aggregate to support multiple sets of radiating stalk cells (100-300 μm in length). *A. eriantha* exhibits directional stalk cell growth exceeding 1000 μm. The hairs of *A. deliciosa* are characterized by typical bristle structures requiring tens to hundreds of basal cells to form epidermal protrusions, resulting in an uneven surface texture. These exhibit diverse growth patterns, including single-branch ('Jinkui'), twin ('Bruno'), and fascicled ('Jinmei') types (Figure 2b).

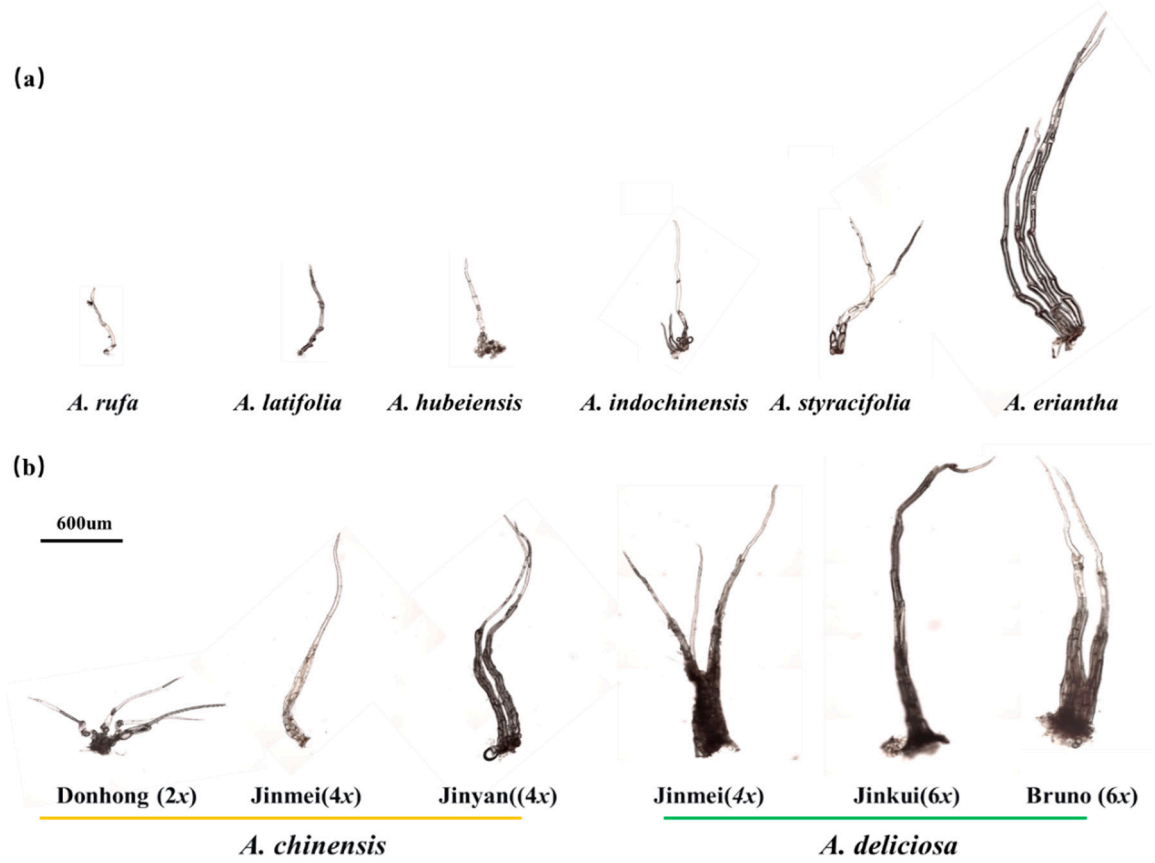

Figure 2. Cytomorphological observation of trichomes in kiwifruit. (a) Morphological and cytological variation of trichomes among different species. (b) Diversity of trichomes in representative diploid (2x), tetraploid (4x), and hexaploid (6x) cultivars of *A. chinensis* and *A. deliciosa*.

 doi:10.20944/preprints202601.2058.v1

3.3. Micromorphological and Density Variation Across Actinidia Taxa

Analysis across the genus revealed significant inter-sectional and inter-specific variation in trichome length, establishing distinct morphological thresholds between taxonomic divisions (Figure 3). Among the 16 species investigated, *A. callosa* var. *henryi* (Sect. *Maculatae*) was uniquely glabrous, whereas other species exhibited high phenotypic plasticity, with lengths ranging from 82.1 μm (*A. callosa* var. *discolor*) to 1084.5 μm (*A. eriantha*). Species within the *Stellatae*/*Strigosae* group (including *A. eriantha*, *A. deliciosa*, and *A. persicina*) formed a distinct statistical cluster characterized by lengths exceeding 1000 μm ($P < 0.05$). Conversely, Sect. *Maculatae* species (e.g., *A. latifolia*) were typically characterized by micro-trichomes (100–350 μm). Interestingly, *A. jiangxigensis* (612.3 μm) appeared to be a morphological intermediate between these two sections (Figure 3a). Furthermore, our data show that trichome density in the *Stellatae* and *Strigosae* sections is consistently higher than in Sect. *Maculatae* (Figure 3b).

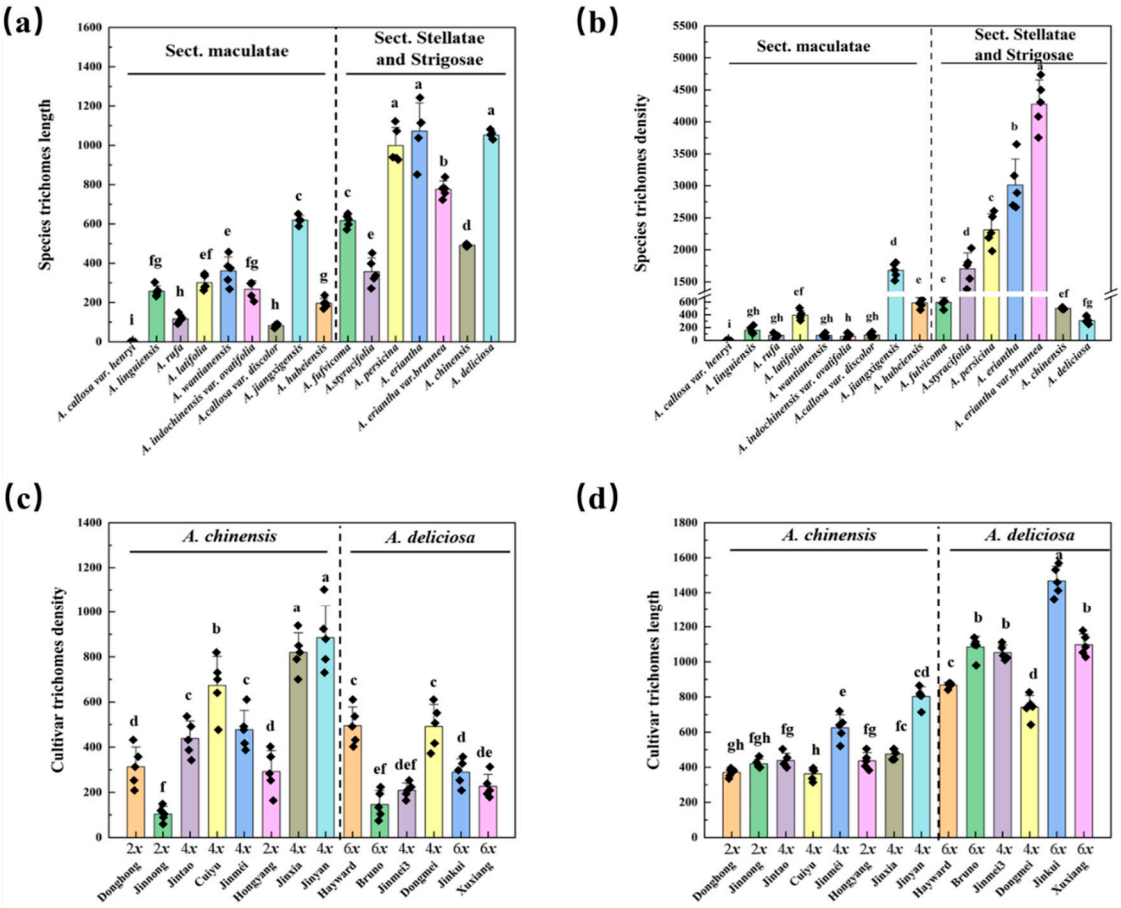

Figure 3. Analysis of trichome micromorphology and density across 16 *Actinidia* species and 14 *A. chinensis* and *A. deliciosa* cultivars.

Quantitative assessment of 14 commercial cultivars across three ploidy levels (2x, 4x, and 6x) revealed a trade-off between trichome density and length (Figure 3). *A. chinensis* cultivars generally exhibited higher average densities than *A. deliciosa*, though the latter produced significantly longer trichomes. Among *A. chinensis* accessions, 'Jinyan' and 'Jinxia' recorded the highest densities (approximately 900 and 820 units/cm², respectively; $P < 0.05$) alongside moderate lengths (450–800 μm). In contrast, *A. deliciosa* cultivars such as 'Jinkui' recorded the greatest lengths (>1400 μm). Significant intra-specific variation was also observed; for instance, the trichome density of *A. chinensis* 'Jinxia' was fivefold that of 'Jinnong'. These findings suggest divergent adaptive strategies: *A. chinensis* prioritizes dense, short-range coverage, whereas *A. deliciosa* invests in elongated, sparse bristles.

 doi:10.20944/preprints202601.2058.v1

3.4. Comparative Analysis of Pericarp Thickness

High-resolution evaluation using paraffin sectioning and SAIViewer software revealed that pericarp thickness is closely aligned with taxonomic sections, with mean values ranging from 59.8μm to 534.6μm (Fig4). Sect. *Leiocarpae*: characterized by a single layer of tightly packed cells, resulting in the thinnest profiles (e.g., *A. arguta* var. *giraldii* approx 59μm (Fig 4a, c). Sect. *Maculatae* exhibited intermediate robustness (369.2μm in *A. callosa* var. *discolor*), featuring stratified cork cells and dense cortical layers. Sect. *Stellatae*/*Strigosae* contained the genus maximum (*A. eriantha*, 534.6μm) (Fig 4a, c), featuring a robust architecture of multiple orderly cell layers.

Among the 14 commercial cultivars, thickness profiles frequently overlapped. 'Jinkui' and 'Xuxiang' (*A. deliciosa*) demonstrated the highest mean thickness (305.4μm and 298.7μm), whereas 'Jinmei' was the thinnest at 126.3 μm (Figure4b, d). In *A. chinensis*, 'Jinyan' and 'Donghong' exhibited robust values (283.5 μm and 265.1μm) (Fig 4b, d). Notably, localized thickening was observed at trichome insertion sites, whereas areas devoid of trichomes were often reduced to a single cell layer. These results indicate that cultivar-level selection is a more critical determinant of skin robustness than species-level classification alone.

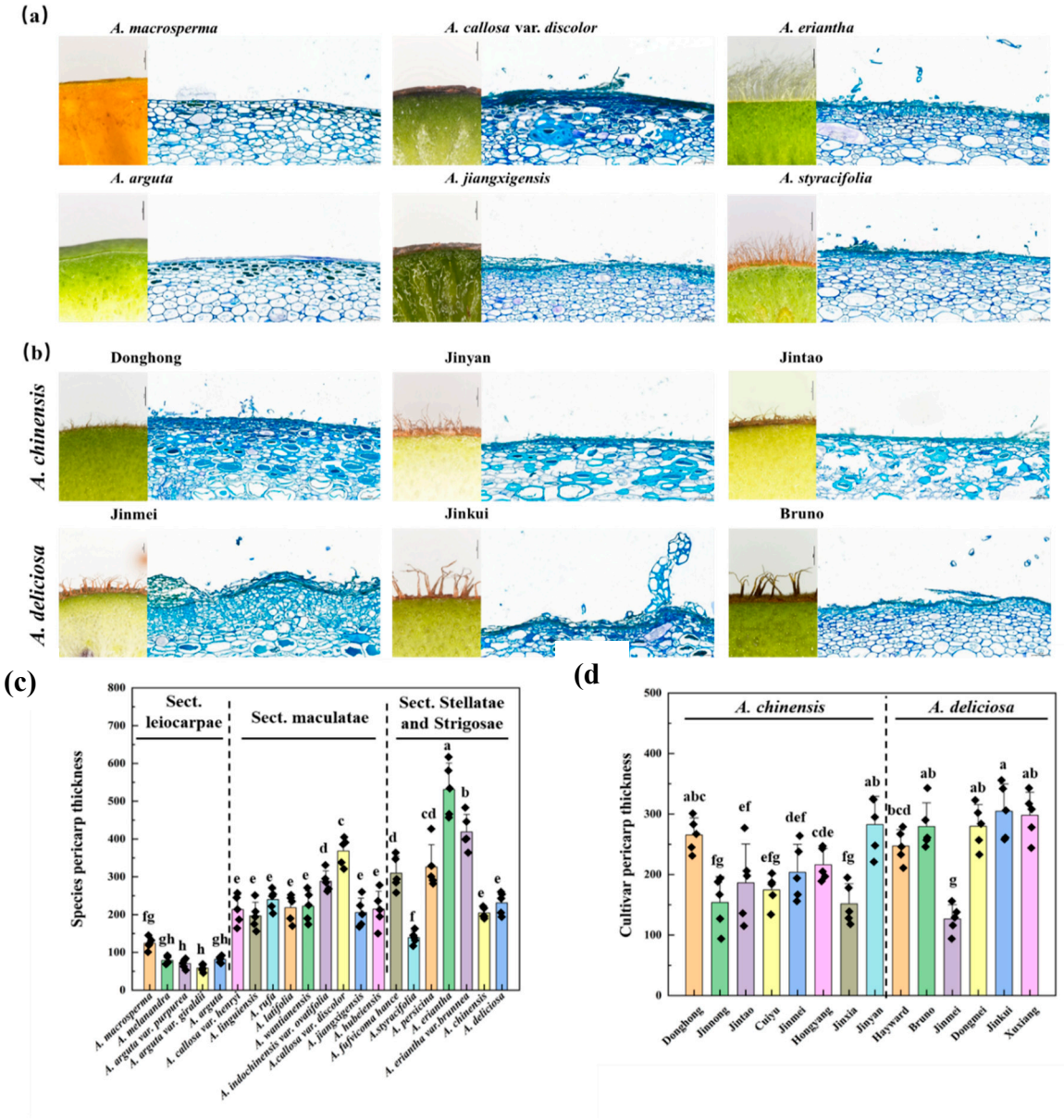

Figure 4. Anatomical observation and comparison of the pericarp in kiwifruit species and cultivars of *A. chinensis* and *A. deliciosa.*

 doi:10.20944/preprints202601.2058.v1

3.5. Transcriptomic Analysis of Ploidy-Induced Trichome Morphogenesis

Correlation analysis between ploidy and pubescence traits revealed that while trichome density showed no significant correlation with ploidy level (R = 0.012), both trichome length and total biomass exhibited a highly significant positive correlation (P < 0.001$, Figure 5a). Consequently, higher ploidy levels result in an increased trichome volume per unit area, making these cultivars appear more densely pubescent.

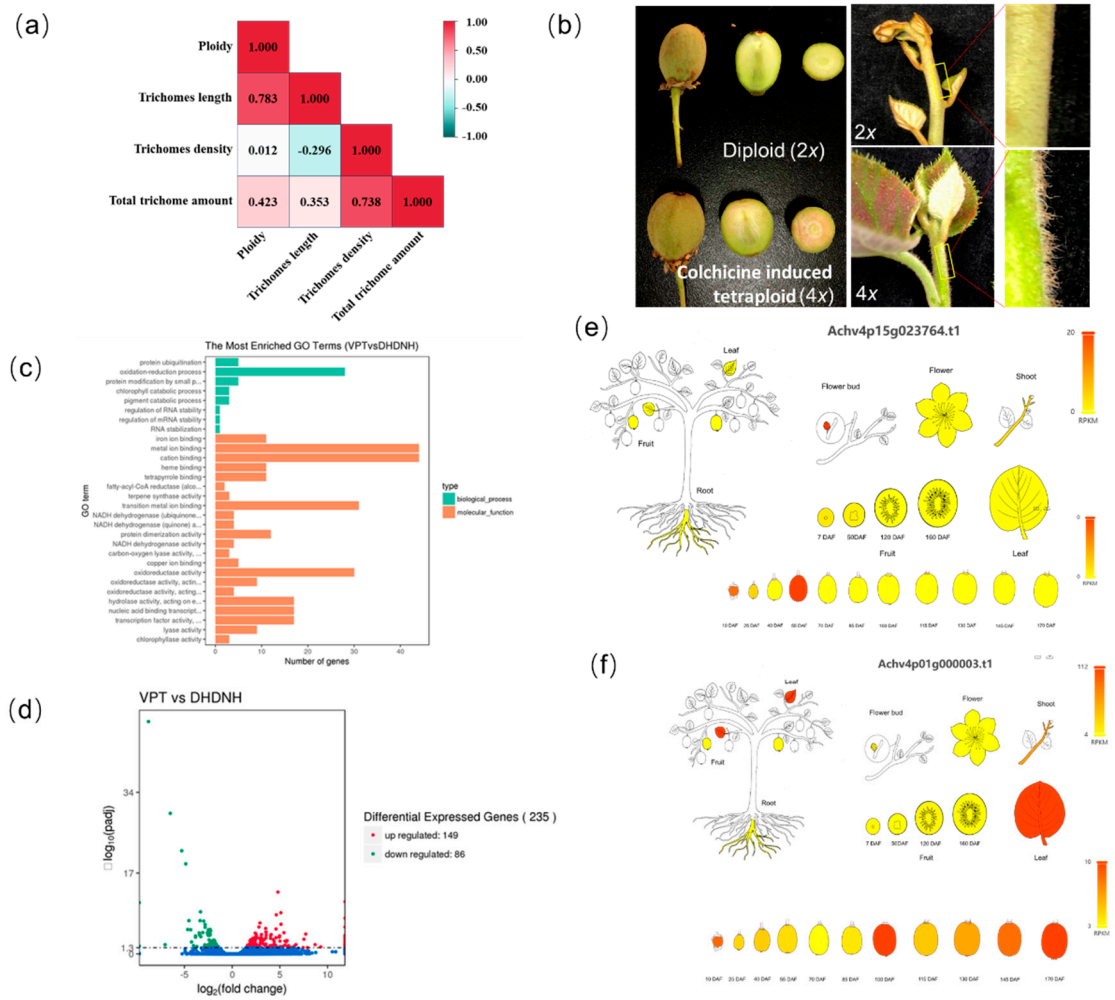

Figure 5. Identification of trichome-related genes using induced polyploidy. (a) Correlation analysis between ploidy and trichome density, length, and amount, (b) Phenotypic differences in fruits, young stems, and trichomes between diploid A. chinensis 'Donghong' and its colchicine-induced autotetraploid counterpart. (c) Bar graph of GO enrichment analysis for differentially expressed genes (DEGs) between diploid and tetraploid kiwifruit. (e) Volcano plot of the DEGs. (e-f) Expression patterns of candidate trichome development genes across various tissues and fruit developmental stages.

To elucidate the genetic basis of these changes, an autotetraploid line was induced from the diploid cultivar 'Donghong' using colchicine. This provided a consistent genetic background to isolate the effects of genome doubling from nucleotide variation. The tetraploid line exhibited pronounced "gigas" effects, with significantly increased trichome length and density across vegetative organs (Figure 5b). Comparative transcriptomic analysis identified 235 differentially expressed genes (DEGs), comprising 149 up-regulated and 86 down-regulated transcripts (Figure 5d). KEGG enrichment analysis highlighted pathways associated with oxidation-reduction processes and cation binding (Figure 5c).

 doi:10.20944/preprints202601.2058.v1

Temporal expression profiling identified two primary candidate genes: *Achv4p15g023764.t1* and *Achv4p01g000003.t1*. *Achv4p15g023764.t1* reached peak expression during the active trichome initiation phase (10–55 days after flowering), suggesting a role in early morphogenesis. Conversely, *Achv4p01g000003.t1* was significantly up-regulated during the late maturation phase (after 100 days), indicating its involvement in the final structural maturation of the trichome. These genes represent promising targets for molecular breeding aimed at optimizing fruit surface characteristics.

4. Discussion

The genus *Actinidia* exhibits an extraordinary spectrum of epidermal variation, ranging from the glabrous surfaces of Section *Leiocarpae* to the dense, persistent tomentum characteristic of Section *Strigosae* [19,20]. This study confirms that kiwifruit trichomes are exclusively multicellular and non-glandular—a structural hallmark that distinguishes them from the unicellular or glandular types prevalent in model species such as *Arabidopsis* [2,3]. Our findings suggest that this bipartite multicellular architecture, consisting of a basal cell cluster and a terminal stalk cell, represents a functional specialization optimized for physical defense rather than chemical secretion. The cytomorphological features of *A. eriantha* provide compelling evidence for this specialization [21]. Furthermore, the significant inter-sectional variation in trichome length and density reflects divergent evolutionary strategies: while *A. chinensis* relies on high-density short hairs for protection, *A. deliciosa* and *A. eriantha* have evolved elongated, rigid structures to form a more robust physical barrier [22].

A critical finding of this study is the localized thickening of the pericarp at trichome insertion sites. The recruitment of multiple cell layers to support the trichome base contributes to the overall structural integrity of the fruit skin, particularly in pubescent species like *A. eriantha* [22]. These results complement the work of Celano et al. (2009) regarding the relationship between kiwifruit peel architecture and water loss [23]. However, this relationship is complex; while the pericarp serves as the primary physical barrier, water loss kinetics are also governed by secondary factors, including cuticle composition, lenticel (spot) density, and internal metabolic activity [18].

Polyploidy, or whole-genome duplication (WGD), is a major driver of phenotypic novelty and environmental adaptation in plants. One of the most prominent effects of polyploidization on plant anatomy is the modification of trichomes—specialized epidermal outgrowths that serve as defense mechanisms and metabolic hubs [24]. Polyploid plants frequently exhibit significantly larger trichomes than their diploid counterparts; for example, in *Melissa officinalis*, tetraploidy results in enlarged peltate trichomes [25], while in *Arabidopsis*, higher ploidy levels are linked to increased trichome branching (Wang et al., 2022). Our investigation of various cultivars and the induced 'Donghong' autotetraploid line provides direct evidence that polyploidization significantly alters trichome phenotypes, enhancing both length and density. This "gigas" effect—a hallmark of polyploidy—may confer a competitive advantage by bolstering the plant's resilience to biotic and abiotic stressors [26].

The transcriptomic identification of candidate genes *Achv4p15g023764.t1* and *Achv4p01g000003.t1* provides a roadmap for future molecular breeding. Their distinct temporal expression patterns—peaking during early initiation and late maturation, respectively—suggest a multi-phase regulatory mechanism governing kiwifruit hair development. Additionally, the RNA-seq data from autotetraploid kiwifruit provide genomic-level evidence for the regulation of trichome-associated genes by polyploidization. Future super pan-genome studies are expected to further elucidate the allelic variation and evolutionary characteristics of these developmental genes [22].

By systematically mapping the diversity of kiwifruit trichomes and pericarp structures, this study bridges the gap between fundamental genomic research and practical horticultural application. The identification of Section *Leiocarpae* as a genetic reservoir for "edible-skin" breeding and the elucidation of the regulatory networks underlying trichome morphogenesis offer strategic guidance for the industry. This systematic mapping provides a foundation for selecting species with distinct pubescence traits for hybridization programs, facilitating the development of novel kiwifruit

 doi:10.20944/preprints202601.2058.v1

germplasm. For instance, varieties with denser trichome coverage and thicker pericarps can be bred to enhance physical defense against environmental stress. Conversely, hybridization with glabrous species such as *A. arguta* could facilitate the development of kiwifruit varieties with edible peels, analogous to apples. Future research utilizing genome-editing technologies to precisely manipulate these candidate genes will be essential for developing next-generation cultivars with optimized surface protection and superior postharvest quality.

Author Contributions: Conceptualization, X.X.; D.Y; methodology, Q.X.; H. F., L.L.; L.H.; X.C.; formal analysis X.X.; Q.X.; D. Y.; writing—original draft preparation, Q.X.; X.X.; E.M.; writing—review and editing, D.Y; X.X.; Z, X.; E.M. All authors have read and agreed to the published version of the manuscript.

Funding: This project was supported by the National Natural Science Foundation of China (32202436) and National Key Research and Development Program of China (2024YFE0214500), CARS(CARS-26) and Hubei Province Natural Science and Technology resource database.

Data Availability Statement: The original contributions presented in this study are included in the article. Further inquiries can be directed to the corresponding author.

Conflicts of Interest: The authors declare that they have no known competing financial interests or personal relationships that could have appeared to influence the work reported in this paper

References

1. Werker, E. Trichome diversity and development. *Advances in Botanical Research*, 2000, 31: 1-35. https://doi.org/10.1016/S0065-2296(00)31005-9.
2. Chalvin, C.; Drevensek, S.; Dron, M.; Bendahmane, A.; Boualem, A. Genetic control of glandular trichome development. *Trends in Plant Science*, 2020, 25(6): 477-487. https://doi.org/10.1016/j.tplants.2019.12.025.
3. Mauricio, R. Costs of resistance to natural enemies in field populations of the annual plant *Arabidopsis thaliana*. *The American Naturalist*, 1998, 152(2): 265-272. https://doi.org/10.1086/286164.
4. Ran, R.; Li, X.; Zhang, J.; Zhao, J.; Zhao, X.; Cui, X.; Chen, G.; Zhao, P. Monocot-like leaf structure and trichome-water relations in early growth stages of the C3 plant sand rice (*Agriophyllum squarrosum*). *Plant Science*, 2025, 112480. https://doi.org/10.1016/j.plantsci.2025.112480.
5. Oksman-Caldentey, K.; Inzé, D. Plant cell factories in the post-genomic era: new ways to produce designer secondary metabolites. *Trends in Plant Science*, 2004, *9*(9), 433–440. https://doi.org/10.1016/j.tplants.2004.07.006.
6. Cao, J.; Zhao, Y.; Tang, K. MYC: orchestrating secondary metabolism and glandular trichome formation. *Trends in Plant Science*, 2025, 30(8), 821–825. https://doi.org/10.1016/j.tplants.2025.03.019.
7. Wang, H.; Ren, J.; Zhou, S.; Duan, Y.; Zhu, C.; Chen, C.; Liu, Z.; Zheng, Q.; Xiang, S.; Xie, Z.; Wang. X.; Chai, J.; Ye, J.; Xu, Q.; Guo, W.; Deng, X.; Zhang, F. (2024). Molecular regulation of oil gland development and biosynthesis of essential oils in *Citrus* spp. *Science*, *383*(6683), 659-666. https:// DOI: 10.1126/science.adl2953
8. Feng, Z.; Bartholomew, E. S.; Liu, Z.; Cui, Y.; Dong, Y.; Li, S.;Wu, H.; Ren, Z.; Liu, X. (2021). Glandular trichomes: new focus on horticultural crops. *Horticulture Research*, *8*. https://doi.org/10.1038/s41438-021-00592-1
9. Fu, Y.; Li, M.; Zhang, W.; Liu, X.; Huang, L.; Zhang, S.; Liang, X.; Zhang, L.; Tang, K.; Jocelyn, K.; Shen, Q. (2025). The role, regulation and application of plant fruit trichomes. *Molecular Horticulture*, *5*(1), 41. https://doi.org/10.1186/s43897-025-00167-x
10. Li, X.; Li, J. (2007). Lectotypification of *Actinidia*. *Nordic Journal of Botany*, *25*(5-6), 294-295. https://doi.org/10.1111/j.0107-055X.
11. Liang, C. The genus *Actinidia* in China. *Beijing: Science Press*, 1984.
12. Wu, M.; Bian, X.; Hu, S.; Huang, B.; Shen, J.; Du, Y.; Wang, Y.; Xu, M.; Xu, H.; Yang, M.; Wu, S. A gradient of the Hd-Zip regulator woolly regulates multicellular trichome morphogenesis in tomato. *The Plant Cell*, 2024, *36*(6), 2375–2392. https://doi.org/10.1093/plcell/koae077.
13. Wu, M.; Bian, X.; Huang, B.; Du, Y.; Hu, S.; Wang, Y.; Shen, J.; Wu, S. (2024). HD-Zip proteins modify floral structures for self-pollination in tomato. *Science*, *384*(6691), 124-130. https:// doi.10.1126/science.adl19

 doi:10.20944/preprints202601.2058.v1

14. Yu, N.; Cai, W.; Wang, S.; Shan, C.; Wang, L.; Chen, X.. Temporal control of trichome distribution by microRNA156-targeted SPL genes in *Arabidopsis thaliana*. *The Plant Cell*, 2010, *22*(7), 2322–2335. doi:10.1105/tpc.109.072579.
15. Wu, H.; Yang, W.; Dong, G.; Hu, Q.; Li, D.; & Liu, J. (2025). Construction of the super pan-genome for the genus Actinidia reveals structural variations linked to phenotypic diversity. *Horticulture Research*, *12*(6), uhaf067. https://doi.org/10.1093/hr/uhaf067
16. Wu, M.; Bian, X.; Hu, S.; Huang, B.; Shen, J.; Du, Y.; Wang, Y.; Xu, M.; Xu, H.; Yang, M.; Wu, S. A gradient of the HD-Zip regulator woolly regulates multicellular trichome morphogenesis in tomato. *The Plant Cell*, 2024, *36*(6), 2375–2392. https://doi.org/10.1093/plcell/koae077.
17. Wu, M.; Bian, X.; Huang, B.; Du, Y.; Hu, S.; Wang, Y.; Shen, J.; Wu, S. (2024). HD-Zip proteins modify floral structures for self-pollination in tomato. *Science*, *384*(6691), 124-130. https:// doi.10.1126/science.adl19
18. Yu, N.; Cai, W.; Wang, S.; Shan, C.; Wang, L.; Chen, X. Temporal control of trichome distribution by microRNA156-targeted SPL genes in *Arabidopsis thaliana*. *The Plant Cell*, 2010, *22*(7), 2322–2335. doi:10.1105/tpc.109.072579.
19. White J. Ontogeny and morphology of ovarian and fruit hairs in kiwifruit. *New Zealand Journal of Botany*, 1986, *24*(3), 403–414. https://doi.org/10.1080/0028825X.1986.10409818.
20. Ferguson, A. (2007). The need for characterization and evaluation of germplasm: kiwifruit as an example. *Euphytica*, *154*(3), 371-382. https://doi.org/10.1007/s10681-006-9188-2
21. Huang, H.; Li, J.; Ferguson, A. The genus *Actinidia*: a review of morphological and taxonomic characteristics [J]. *Plant Diversity and Resources*, 2013, 35 (6): 697-706.
22. Qi, B.; Li, P.; Li, J.; Zha, M.; Wang, F. (2025). Kiwifruit Peelability (*Actinidia* spp.): A Review. *Horticulturae*, *11*(8), 927. https://doi.org/10.3390/horticulturae11080927
23. Celano, G.; Minnocci, A.; Sebastiani, L.; D'Auria, M.; Xiloyannis, C. Changes in the structure of the skin of kiwifruit in relation to water loss. *The Journal of Horticultural Science and Biotechnology*, 2009, 84(1), 41–46. https://doi.org/10.1080/14620316.2009.11512477.
24. Wei, N.; Cronn, R.; Liston, A.; Ashman, T. (2018). Functional trait divergence and trait plasticity confer polyploid advantage in heterogeneous environments. *New Phytologist*, *221*(4), 2286-2297. https://doi.org/10.1111/nph.15508
25. Bharati, R.; Gupta, A.; Novy, P.; Severová, L.; Šrédl, K.; Žiarovská, J.; & Fernández-Cusimamani, E. (2023). Synthetic polyploid induction influences morphological, physiological, and photosynthetic characteristics in *Melissa officinalis* L. *Frontiers in Plant Science*, *14*. https://doi.org/10.3389/fpls.2023.1332428
26. Wu, J.; Ferguson, A.; Murray, B.; Jia, Y.; Datson, P.; Zhang, J. Induced polyploidy dramatically increases the size and alters the shape of fruit in *Actinidia chinensis*. *Annals of Botany*, 2012, 109(1), 169–179. https://doi.org/10.1093/aob/mcr256.